

# The effects of neutron radiation on shape memory properties and oxidation behaviour of a Cu–13Al–4Ni alloy

C. Tatar<sup>a,\*</sup>, R. Zengin<sup>b</sup>

<sup>a</sup> *Firat University, Faculty of Arts and Sciences, Department of Physics, 23169 Elazig, Turkey*

<sup>b</sup> *Firat University, Faculty of Education, Department of Primary Education, 23169 Elazig, Turkey*

Received 13 April 2007; received in revised form 24 July 2007; accepted 25 July 2007

Available online 30 August 2007

## Abstract

The reverse and forward transformation temperatures and oxidation behavior of neutron irradiated CuAlNi shape memory alloy have been investigated. The alloy was irradiated for 3.6 and 7.2 ks with thermal neutron flux at  $8 \times 10^{12} \text{ n cm}^{-2} \text{ s}^{-1}$ ,  $E > 1 \text{ MeV}$ .

It was seen from differential scanning calorimetry (DSC) that the forward and reverse transformation temperatures of the martensite  $\leftrightarrow$  austenite were decreased with the applied radiation. Enthalpies of transformation ( $\Delta H$  heating and  $\Delta H$  cooling) increase with neutron irradiation. Thermogravimetric measurements were carried out to investigate the kinetics of oxidation. The activation energy of oxidation for alloy was calculated using thermogravimetric data.

© 2007 Elsevier Masson SAS. All rights reserved.

**Keywords:** Shape memory; Thermal conduction; Heat capacity; Thermal treatment

## 1. Introduction

Smart materials such as shape memory alloys (SMA) have attracted attention in recent years [1–6] and they are expected to be used in nuclear reactor environment. Many researches have examined the stability of their mechanical properties during neutron irradiation. The studies revealed that irradiation affect mechanical, microstructure, and transformation temperatures of the shape memory alloys [7–12]. The influence of oxidation on the mechanical behavior of the shape memory has not thoroughly been investigated. In these investigations, two aspects of oxidation are shown to be of importance. The formation of an oxide scale on the shape memory alloy surface can be calculated on the basis of diffusion coefficients and activation energy of oxidation a period.

It is important to clarify the effects of various irradiation and oxidation conditions. The aim of this study is to investigate the effect of the irradiation on transformations and oxidation behavior of Cu–13Al–4Ni alloy.

## 2. Experimental

The chemical composition of the alloy used for this work was Cu–13Al–4Ni (in wt pct), and the  $e/a$  ratio is 1.55. The alloy was supplied by the Scientific and Technical Research Council of Turkey. Bulk specimens for investigations were solution-treated in the  $\beta$ -phase region (for 30 minutes  $930^\circ\text{C}$ ) and immediately quenched in iced brine to obtain the B-type martensitic structures. Neutron irradiation was then performed on the samples at Istanbul Technical University, Institute of Nuclear Energy. The thermal neutron flux is  $8 \times 10^{12} \text{ n cm}^{-2} \text{ s}^{-1}$ . The specimens were irradiated for 3.6 and 7.2 ks.

In order to determine the transformation energies and the forward and reverse transformation temperatures, disc shaped specimens of 80, 74, and 82 mg from alloys unirradiated, and than irradiated for 3.6 and 7.2 ks respectively, were a period. The calorimetric experiments were performed by means of a computer-controlled Shimadzu DSC-50 instrument at a rate of  $10^\circ\text{C min}^{-1}$  between 20 and  $190^\circ\text{C}$ . The cooling treatments were performed using liquid nitrogen.

In order to determine the increase in mass at free atmosphere, the piece specimens 45.3, 35.6, and 43.7 mg from the alloys unirradiated, irradiated for 3.6 kilosecond (ks), and

\* Corresponding author.

E-mail address: [ctatar@firat.edu.tr](mailto:ctatar@firat.edu.tr) (C. Tatar).

irradiated for 7.2 ks alloys were heated and cooled, respectively. The experiments for this purpose were performed by means of a computer-controlled Shimadzu TGA-50 instrument at a of  $10^\circ\text{C min}^{-1}$  heating and cooling rate.

### 3. Results and discussion

#### 3.1. The effect of neutron treatment on transformation temperatures of the alloy

Fig. 1 shows the differential scanning calorimetry curves of unirradiated [13] and neutron-irradiated alloy. The transformation temperatures, i.e. the martensite transformation start ( $M_s$ ), finish temperatures ( $M_f$ ) and austenite transformation start ( $A_s$ ), finish temperatures ( $A_f$ ), have been determined from the curves and enthalpies values for unirradiated and neutron-irradiated treatments are given in Tables 1–3. The DSC peaks on each curve depend on the inverse martensitic transformation when these are the curves generated during from the heating process. It is seen from figure that the peaks for austenite transformation are slightly shifted from their initial positions to lower temperatures. This indicates that the energy of irradiation-induced atomic displacements may be harnessed to produce a number of different phase transformations. Irradiation-induced defects increase the diffusion coefficient and give a phase transformation at temperatures where they normally do not occur. Irradiation also produces vacancies and interstitials in this alloy. It is also found that irradiation introduces amorphization in the alloy. The amorphization is a topological disorder since it would make the degree of Bragg–Williams order decrease, and the peak can shift to lower temperatures [14]. Topological disorder is the lateral disorder in which atoms are located at random positions in space. When the irradiated DSC curves are compared with one another, it is seen that the intensity of the DSC peak is a decreased by irradiation. Thus, decrease in the intensity of peak would correspond to the amount of the martensite transformation and amount of amorphous phase. It is evaluated that the amorphous phase was observed after irradiation and DSC peak decreased in intensity with a slight shifting to lower temperatures. DSC revealed that  $A_f$  transformation temperatures for 3.6 and 7.2 ks irradiated alloy follows the order  $A_fC1 > A_fC2 > A_fC3$ .  $M_s$ , transformation temperatures for 3.6 and 7.2 ks irradiated alloy are also found to be  $M_sC3 > M_sC2 > M_sC1$  and  $M_sC3 > M_sC2 > M_sC1$ , respectively. The austenite and martensite transformation temperatures for first, second, third cycles are named as  $A_fC1, A_fC2, A_fC3$  and  $M_sC1, M_sC2, M_sC3$ , respectively.

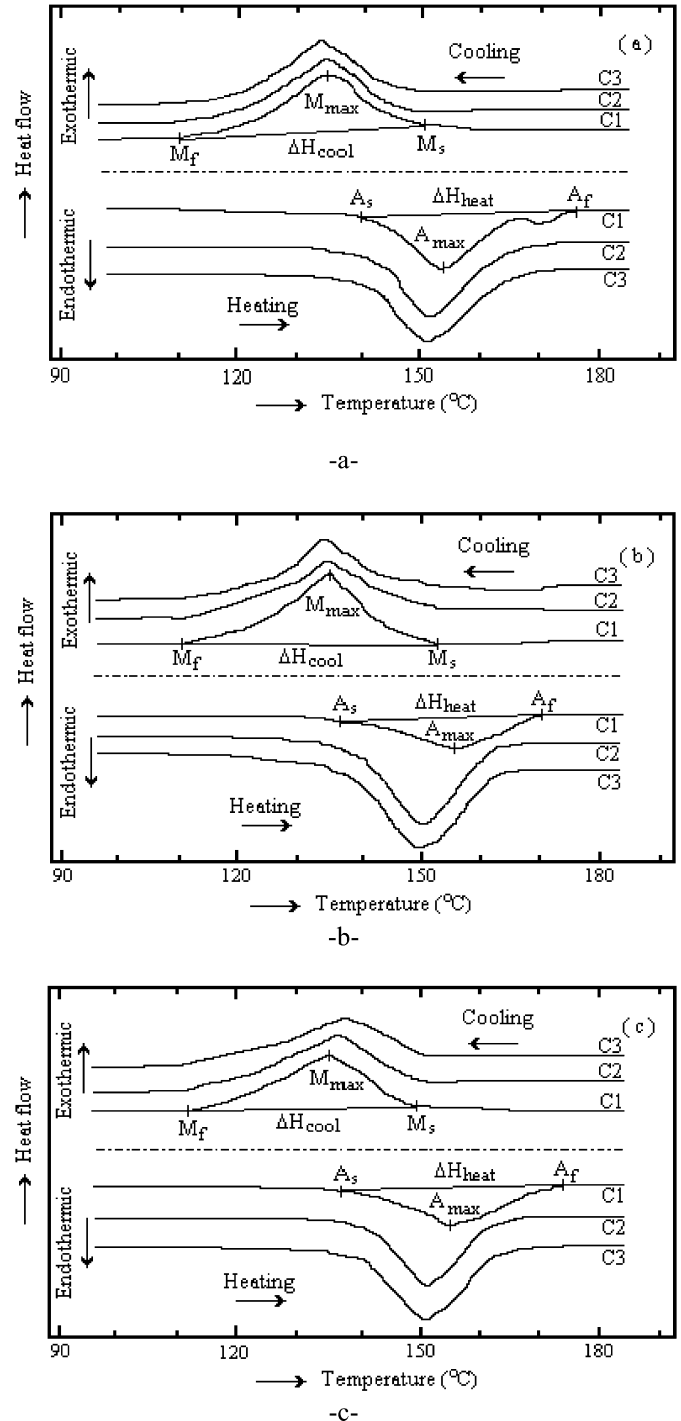


Fig. 1. DSC curves of the alloy: (a) thermal treatment [13], (b) neutron treatment for 3.6 ks, (c) neutron treatment for 7.2 ks.

Table 1  
Transformation temperatures and enthalpy values of unirradiated [13] alloy

Unirradiated	$A_s$ ( $^\circ\text{C}$ )	$A_{\text{max}}$ ( $^\circ\text{C}$ )	$A_f$ ( $^\circ\text{C}$ )	$M_s$ ( $^\circ\text{C}$ )	$M_{\text{max}}$ ( $^\circ\text{C}$ )	$M_f$ ( $^\circ\text{C}$ )	$\Delta H_{\text{heat}}$ ( $\text{J g}^{-1}$ )	$\Delta H_{\text{cool}}$ ( $\text{J g}^{-1}$ )
C1	139.9	155.1	176.3	150.6	135.8	110.1	-5.91	6.20
C2	135.8	153.1	172.3	150.6	135.8	110.1	-6.49	6.51
C3	135.4	152.3	172.5	150.9	133.5	112.7	-6.45	6.42

Table 2  
Transformation temperatures and enthalpy values of irradiated alloy for 3.6 ks

Irradiated for 3.6 ks	$A_s$ (°C)	$A_{max}$ (°C)	$A_f$ (°C)	$M_s$ (°C)	$M_{max}$ (°C)	$M_f$ (°C)	$\Delta H_{heat.}$ (J g <sup>-1</sup> )	$\Delta H_{cool.}$ (J g <sup>-1</sup> )
C1	137.4	154.7	171.4	153.0	135.8	112.4	-5.49	7.21
C2	135.8	150.6	167.7	153.7	135.0	111.4	-8.03	5.97
C3	135.4	149.7	166.1	153.9	134.3	110.7	-7.86	6.68

Table 3  
Transformation temperatures and enthalpy values of irradiated alloy for 7.2 ks

Irradiated for 7.2 ks	$A_s$ (°C)	$A_{max}$ (°C)	$A_f$ (°C)	$M_s$ (°C)	$M_{max}$ (°C)	$M_f$ (°C)	$\Delta H_{heat.}$ (J g <sup>-1</sup> )	$\Delta H_{cool.}$ (J g <sup>-1</sup> )
C1	137.1	154.2	174.4	148.9	135.6	113.6	-5.30	9.27
C2	135.2	152.4	168.7	149.4	138.2	112.4	-7.57	7.09
C3	134.3	151.8	167.5	149.7	138.8	111.7	-8.07	7.19

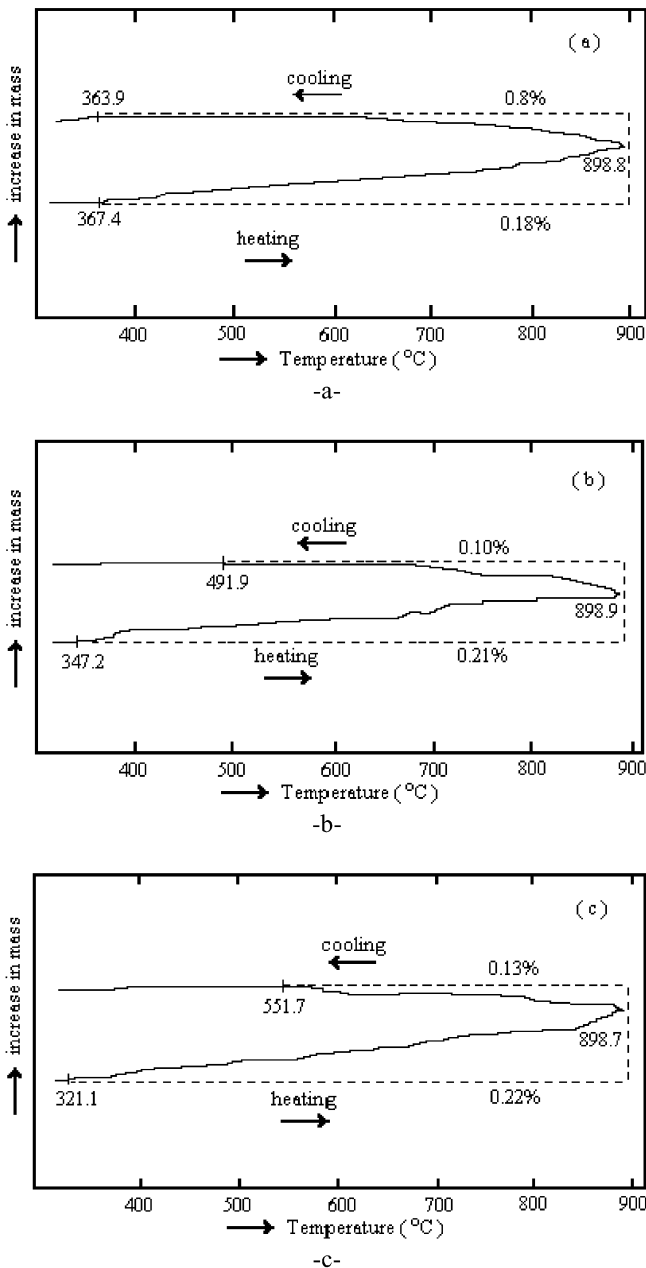


Fig. 2. TGA curves of the alloy for heating and cooling cycles: (a) thermal treatment, (b) neutron treatment for 3.6 ks, (c) neutron treatment for 7.2 ks.

Table 4  
Activation energy and pre-exponential constant values of oxidation

	$E$ (kJ mol <sup>-1</sup> )	$\ln K_o$
Unirradiated	29.3	-2.06
Irradiated for 3.6 ks	20.49	-2.91
Irradiated for 7.2 ks	23.2	-2.56

3.2. The effect of neutron treatment on oxidation behavior of the alloy

Fig. 2(a)–(c) shows TGA curves of treated alloy. The alloy was subjected to thermal treatment and neutron treatment for 3.6 and 7.2 ks. It is seen that mass gain in the TGA curves gradually with increasing temperature. The plots of (weight gain)<sup>2</sup> vs temperature are given in Fig. 3. The oxidation kinetics curves determined as function of the temperature have a roughly linear shape. The rate law can be expressed under the form of a separate the variables expression [15],

$$v = \frac{d\alpha}{dt} = f(\alpha)g(p)h(T) = K_p K_T f(\alpha) P^n \exp\left(-\frac{E}{RT}\right) \quad (1)$$

where  $f(\alpha)$  is a morphological term characteristic of reaction area. The diffusional oxidation process is a thermal activated process. The temperature dependence of the oxidation rate constant is shown in Fig. 2. The temperature dependence of the oxidation rate constant is expressed by the following relation [16],

$$K_p = K_o \exp\left[-\frac{E}{RT}\right] \quad (2)$$

where  $K_o$  is the pre-exponential constant,  $E$  is the activation energy,  $R$  is the gas constant and  $T$  is the temperature. The oxidation rate for alloy is plotted as a function of temperature, as shown in Fig. 4. The activation energies and pre-exponential constant values for the alloy are calculated and given in Table 4. The comparison of calculated energies of oxidation was found to be  $E_{unir} > E_{ir7.2ks} > E_{ir3.6ks}$ .

4. Conclusions

The reverse and forward transformation temperatures and oxidation behavior of neutron irradiated CuAlNi shape memory

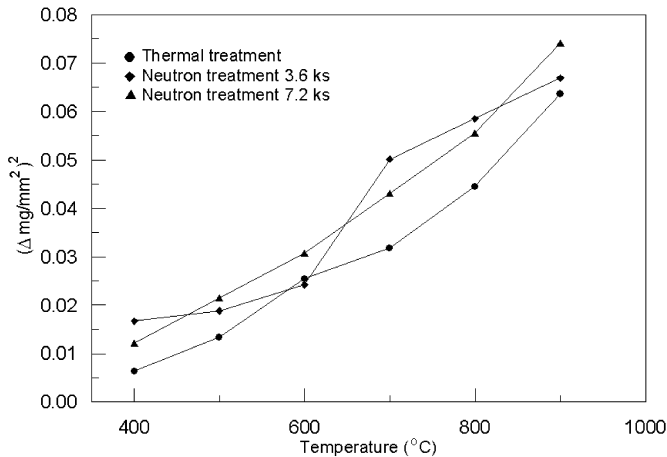


Fig. 3. The variation of  $(\Delta \text{mg mm}^{-2})^2$  with temperature.

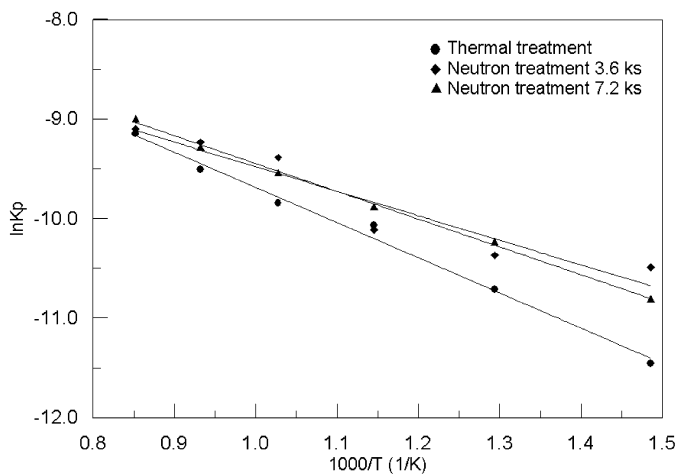


Fig. 4. Oxidation rate constant as a function of temperature for alloy.

alloy have been investigated. The reverse and forward transformation temperatures  $A_s$ ,  $A_{\text{max}}$  (max. temperatures of transformation to austenite),  $A_f$ ,  $M_s$ ,  $M_{\text{max}}$  (max. temperatures of transformation to martensite),  $M_f$ , absorbed and released energies  $\Delta H$  heating,  $\Delta H$  cooling obtained from the curves are given in Tables 1–3. It has been observed that these tempera-

tures decrease in the following cycles. In addition, the applications of neutron irradiation onto the samples have affected the movements of atoms and the displacement of atoms becomes more difficult. Because of the difficulty of this atomic mobility and increasing number of point defects, the transformation temperatures have decreased. This decrease of the reverse transformation temperatures can be attributed to the dislocations formed by the cycling effect and it means that the alloy has the most stable state at the as-quenched case and loses the stability with further cycles [12,17,18]. Enthalpies of transformation ( $\Delta H$  heating and  $\Delta H$  cooling) increase with irradiation. TGA curve taken for irradiated specimens is shown in Fig. 2. During the heating and cooling periods the mass gain of the Cu–Al–Ni alloy may be explained by oxidation.

## References

- [1] R. Stalmans, J. Van Humbeeck, L. Delaey, *Acta Metall. Mater* 40 (1992) 501.
- [2] F.C. Lowey, V. Toma, *Prog. Mater. Sci.* 44 (1999) 189.
- [3] G.L. Geng, Y.J. Bai, S.H. Wang, *Mater. Charact.* 42 (1999) 45.
- [4] Z.G. Wei, R. Sandstrom, *J. Mater. Sci.* 33 (1998) 3743.
- [5] Y.J. Bai, Q.Q. Shi, D.S. Sun, X.F. Bian, G.L. Geng, *J. Mater. Sci. Lett.* 18 (1999) 1509.
- [6] Y.J. Bai, Y.X. Liu, D.S. Sun, X.F. Bian, L.M. Xiao, G.L. Geng, *Mater. Lett.* 46 (2000) 358.
- [7] M. Nishikawa, T. Narikawa, M. Iwamoto, K. Watarabe, *Fusion Technol.* 9 (1986) 101.
- [8] A. Kimura, H. Tsuruga, M. Morimura, S. Miyanaki, J. Misawa, *Mater. Trans. JIM* 34 (1993) 1076.
- [9] T. Hoshiya, F. Takada, M. Omi, I. Guto, H. Ando, *J. Japan Inst. Met.* 56 (1992).
- [10] Y. Matsukawa, T. Suda, S. Ohnuki, C. Namba, *J. Nuclear Mater.* 27 (1999) 106.
- [11] C. Tatar, *Thermochim. Acta.* 437 (2005) 121–125.
- [12] C. Tatar, R. Zengin, *Mater. Lett.* 59 (2005) 3304–3307.
- [13] R. Zengin, S. Ozgen, M. Ceylan, *Thermochim. Acta* 414 (2004) 79–84.
- [14] S. Banerjee, K. Urban, *Phys. Stat. Sol A* 81 (1984) 45.
- [15] B. Gillot, M.E. Guendouzi, M. Laarj, *Mater. Chem. Phys.* 70 (2001) 56.
- [16] T.C. Wang, R.Z. Chen, W.H. Tuan, *J. Europ. Ceram. Soc.* 23 (6) (2003) 927–934.
- [17] C.M. Friend, *Scr. Metall.* 20 (1986) 213.
- [18] J. Perkins, W.E. Muesing, *Metall. Trans. A, Phys. Metall. Mater. Sci. A* 14 (1983) 33.